INTERNATIONAL JOURNAL FOR NUMERICAL METHODS IN FLUIDS
Int. J. Numer. Meth. Fluids **31**: 345–358 (1999)

FINITE ELEMENTS FOR CFD—HOW DOES THE THEORY COMPARE?

A.J. BAKER[a,*], D.J. CHAFFIN[b,1], J.S. IANNELLI[b,2] AND S. ROY[c,3]

[a] *Engineering Science Program, MAES Department, 316A Perkins Hall, University of Tennessee, Knoxville, TN 37996-2030, USA*
[b] *The University of Tennessee, Knoxville, TN 37996-2030, USA*
[c] *J.I. Case Corporation, Burr Ridge, IL, USA*

SUMMARY

The quest continues for accurate and efficient computational fluid dynamics (CFD) algorithms for convection-dominated flows. The boundary value 'optimal' Galerkin weak statement invariably requires manipulation to handle the disruptive character introduced by the discretized first-order convection term. An incredible variety of methodologies have been derived and examined to address this issue, in particular, seeking achievement of monotone discrete solutions in an efficient implementation. The UT CFD research group has participated in this search, leading to the development of consistent, encompassing theoretical statements exhibiting quality performance, including generalized Taylor series (Lax–Wendroff) methods, characteristic flux resolutions, subgrid embedded high-degree Lagrange bases and assembled stencil optimization for finite element weak statement implementations. For appropriate model problems, recent advances have led to accurate monotone methods with linear basis efficiency. This contribution highlights the theoretical developments and presents quantitative documentation of achieved high-quality solutions. Copyright © 1999 John Wiley & Sons, Ltd.

KEY WORDS: finite elements; CFD; Galerkin boundary value; accuracy; convergence

1. INTRODUCTION

The computational fluid dynamics (CFD) conservation law system for state variable $q = q(x_j, t)$ is

$$\mathscr{L}(q) = \frac{\partial q}{\partial t} + \frac{\partial}{\partial x_j}(f_j - f_j^v) - s = 0 \quad \text{on } \Omega \times t \subset \Re^n \times \Re^+, \quad 1 \le j \le n, \tag{1}$$

where $f_j = f(u_j, q)$ and $f_j^v = f(\varepsilon\, \partial q/\partial x_j)$ are the kinetic and dissipative flux vectors respectively, the convection velocity is u_j, $\varepsilon > 0$ is the diffusion coefficient that varies parametrically and s is a source. Appropriate initial and boundary conditions close system (1) for the well-posed statement.

* Correspondence to: Engineering Science Program, MAES Department, 316A Perkins Hall, University of Tennessee, Knoxville, TN 37996-2030 USA. E-mail: ajbaker@cfdlab.engr.utk.edu
[1] E-mail: chaffin@lasl.gov
[2] E-mail: jiannell@utk.edu
[3] E-mail: rsubrata@casecorp.com

CCC 0271–2091/99/170345–14$17.50

Computational difficulties occur as $\varepsilon \to 0$, leading to the occurrence of 'thin layer' solutions containing large gradients, e.g. boundary layer, shock. In CFD, this is the natural occurrence for Reynolds number becoming large. Thereby, even though the analytical solution to (1) remains smooth, monotone and bounded, the spatially discretized CFD solution process becomes dominated by an oscillatory error mode, leading to instability in the presence of the Navier–Stokes non-linearity inherent in f_j.

Thus, a CFD algorithm research goal is an efficient, multi-dimensional 'arbitrary' grid algorithm extracting an accurate, stable and monotone solution for (1) on a *practical mesh* for arbitrary ε. A favourite stabilizing technique is artificial viscosity [1–3] and/or flux correction operations [4,5] containing one or more arbitrary parameters. Flux vector splitting methods [6] replace parameters with switches, but solutions may still exhibit oscillations near strictly local extrema. Implementation of non-linear correction factors called *limiters* [7] requires a relatively dense mesh for interpolation to attain an essentially non-oscillatory (ENO) solution. Finally, these theories are developed via one-dimensional schemes, and hence become theoretically tedious in a multi-dimensional application.

'Intelligent' algorithms for handling solution mesh adaptation in an *automatic* manner have been extensively examined in finite element (FE) solution-adaptive '*p* and *hp*' forms [8–14]. Several advantages, including 'unstructured meshing,' accrue to these algorithms, but at a significant cost in increased algorithm operation count and storage requirements that can hinder achieving *practical mesh* solutions. Recent developments in the area of subgrid-scale resolution include hierarchical (*hp*) elements [15] and the inclusion of nodeless bubble functions [16]. Solution monotonicity is typically not an ingredient in these theories, and as the degrees of freedom (DOF) number increase, especially for three-dimensional cases, the algebraic system matrix order increases rapidly, hence, the computer resource requirement also increases. Numerical linear algebra efficiency issues then also become a central issue.

This invited paper summarizes developed weak statement theory and documents performance for verification and benchmark problem statements belonging to the Navier–Stokes problem class.

2. THE WEAK STATEMENT FORMULATION

The 'weak statement' underlies the vast majority of CFD algorithms. The associated integral constraint associated with (1) is

$$\int_\Omega w\left[\frac{\partial q}{\partial t}+\frac{\partial}{\partial x_j}\left(f_j-f_j^v\right)-s\right]\mathrm{d}\Omega=0, \tag{2}$$

where w is any 'admissible' test function. Thereafter, an FE spatial semi-discretization employs the mesh $\Omega^h=\cup_e\Omega_e$, with Ω_e the generic computational domain. The associated FE weak statement implementation for (1) and (2) employs the approximation

$$q(\mathbf{x},t)\approx q^h(\mathbf{x},t)=\bigcup_e q_e(\mathbf{x},t), \tag{3}$$

$$q_e(\mathbf{x},t)=\{N_k(\mathbf{x})\}^T\{Q(t)\}_e, \tag{4}$$

where $\{\cdot\}$ denotes a column matrix, and the trial space FE basis $\{N_k(\mathbf{x})\}$ typically contains Lagrange polynomials complete to degree k, plus perhaps 'bubble functions' [16]. The resultant FE implementation via a Green–Gauss theorem is [17]

$$WS^h = S_e\left(\int_{\Omega^h}\{N_k\}\left(\frac{\partial q^h}{\partial t}-s\right)\mathrm{d}\tau-\int_{\Omega^h}\frac{\partial\{N_k\}}{\partial x_j}(f_j-f_j^\nu)^h\,\mathrm{d}\tau+\oint_{\partial\Omega_e\cap\partial\Omega^h}\{N_k\}(f_j-f_j^\nu)^h\hat{n}_j\,\mathrm{d}\sigma\right), \tag{5}$$

where S_e symbolizes 'assembly' of local (element) coefficients into global arrays, and the surface integral contains (unknown) boundary fluxes for Dirichlet (fixed) boundary conditions.

For all dimensions n of Ω, Equation (5) yields an ordinary differential equation (ODE) system

$$WS^h = [\mathbf{M}]\{Q(t)\}' + \{\mathbf{R}Q\} = 0. \tag{6}$$

Here, $\{Q(t)\}'$ denotes $\mathrm{d}\{Q\}/\mathrm{d}t$, and (6) defines the time derivative necessary to evaluate a temporal Taylor series (TS), e.g. the θ implicit one-step Euler family,

$$\{Q(t_{n+1})\} \equiv \{\mathbf{Q}\}_{n+1} = \{\mathbf{Q}\}_n - \Delta t[\mathbf{M}]^{-1}(\theta\{\mathbf{R}Q\}_{n+1} + (1-\theta)\{\mathbf{R}Q\}_n) + \text{H.O.T.}, \tag{7}$$

where subscript n denotes time level. Clearing $[\mathbf{M}]^{-1}$ and collecting terms to a homogeneous form produces the 'solvable' (non-linear) terminal algorithm statement

$$\{\mathbf{F}Q\} = [\mathbf{M}]\{Q_{n+1} - Q_n\} + \Delta t(\theta\{\mathbf{R}Q\}_{n+1} + (1-\theta)\{\mathbf{R}Q\}_n) = \{0\}. \tag{8}$$

The *Newton algorithm* for the solution of (8) involves the processes

$$[\text{JAC}]\{\delta Q\}^{p+1} = -\{\mathbf{F}Q\}_{n+1}^p, \tag{9a}$$

$$\{Q\}_{n+1}^{p+1} \equiv \{Q\}_{n+1}^p + \{\delta Q\}^{p+1} = Q_n + \sum_{i=1}^{p}\{\delta Q\}^{i+1}, \tag{9b}$$

$$[\text{JAC}] = \frac{\partial\{\mathbf{F}Q\}}{\partial\{Q\}} = [\mathbf{M}] + \theta\Delta t\left(\frac{\partial\{\mathbf{R}Q\}}{\partial\{Q\}}\right). \tag{9c}$$

3. STABILITY, THE TAYLOR WEAK STATEMENT

The UT CFD group research focus [1,18,24] has generalized the methods of Lax and Wendroff [19] and Donea [20], as the Taylor weak statement (TWS). For Equation (1), with $A_j \equiv \partial f_j/\partial q$ as the kinetic flux vector Jacobian, the inviscid form is

$$L(q) = \frac{\partial q}{\partial t} + A_j\frac{\partial q}{\partial t_j} = 0. \tag{10}$$

Temporal derivatives are taken in the manner of Lax–Wendroff, convex combinations of which admit arbitrary weightings, hence

$$\begin{aligned}\frac{\partial^2 q}{\partial t^2} &= \alpha\left(A_j\frac{\partial}{\partial x_j}\frac{\partial q}{\partial t}\right) + \beta\left(A_k\frac{\partial}{\partial x_k}\left(A_j\frac{\partial q}{\partial x_j}\right)\right),\\ \frac{\partial^3 q}{\partial t^3} &= \gamma\left(A_k\frac{\partial}{\partial x_k}\left(A_j\frac{\partial q}{\partial x_j}\frac{\partial q}{\partial t}\right)\right) + \mu\left[A_l\frac{\partial}{\partial x_l}\left(A_k\frac{\partial}{\partial x_k}\left(A_j\frac{\partial q}{\partial x_j}\right)\right)\right],\end{aligned} \tag{11}$$

which when substituted into an explicit Taylor time series [1] and then substituted into (4) yields the 'Taylor series-modified' semi-discrete form

$$\mathscr{L}^m(q) = \mathscr{L}(q) - \frac{\Delta t}{2}\frac{\partial}{\partial x_j}\left[\alpha A_j \frac{\partial q}{\partial t} + \beta A_j A_k \frac{\partial q}{\partial x_k}\right] - \frac{\Delta t^2}{6}\frac{\partial}{\partial x_j}\left[\gamma A_j A_k \frac{\partial q}{\partial x_k}\frac{\partial q}{\partial t} + \mu A_j \frac{\partial}{\partial x_l}\left(A_k \frac{\partial}{\partial x_l}\left(A_l \frac{\partial q}{\partial x_l}\right)\right)\right], \tag{12}$$

where $\mathscr{L}(q)$ remains as defined in (1).

A wide range of independently derived, dissipative Galerkin weak statement algorithms belong to the TWS family for specific linearizations and $(\alpha, \beta, \gamma, \mu)$ selections in (12). In one-dimensional cases, 16 such algorithms are documented in [1]. The extension to multi-dimensional forms, and the QUICK finite volume family is reported in [18], and to complete incompressible Navier–Stokes forms in [24]. The familiar trade names include streamline–upwind Petrov–Galerkin (SUPG), Taylor Galerkin (TG) and least-squares (LS). Each selects $\mu = 0$, since two spatial derivatives do not exist in a linear basis implementation. Generally speaking, LS retains all remaining terms, TG retains the β and γ terms and SUPG retains the α and β terms.

For incompressible flow applications, the kinetic flux vector Jacobian matrix product is approximated as the diagonal matrix $[A_j\ A_k] \approx [u_j\ u_k]$. The TWS β term can then be conveniently combined into the dissipative flux vector yielding (1) in the form

$$\mathscr{L}^m(q) = \mathscr{L}(q) - \frac{\Delta t}{2}\frac{\partial}{\partial x_j}\left(\beta u_j u_k \frac{\partial q}{\partial x_k}\right) \equiv \frac{\partial q}{\partial t} + \frac{\partial}{\partial x_j}(f_j - f_j^m) - s = 0, \tag{13}$$

with the β dissipation residing in the TWS-modified dissipative flux vector

$$f_j^m \equiv \left\{\frac{1}{Re}(1 + C_q Re^{\mathrm{t}})\frac{\partial q}{\partial x_j} + \frac{\beta \Delta t}{2} u_j u_k \frac{\partial q}{\partial x_k}\right\}, \tag{14}$$

where Re is the Reynolds number, C_q is the appropriate TKE model constant set, and $Re^{\mathrm{t}} \equiv \mathbf{v}^{\mathrm{t}}/\nu$, the ratio of turbulent to laminar kinemetic viscosity, is the turbulent Reynolds number.

The TWS γ term is similarly a dissipative operator; however, it resides solely as a time derivative augmentation in the Newton Jacobian side of the penultimate algebraic statement. For time-accurate simulations, the γ term is effective for improved phase accuracy; conversely, it is of no consequence in obtaining a steady state solution.

It is sometimes required, e.g. SUPG, to replace the TWS factor Δt by a length scale. Through the definition of the scalar, multi-dimensional Courant number $C \equiv |\mathbf{u}|(\Delta t/h)$, where $|\mathbf{u}|$ is velocity magnitude and h is a local mesh measure, Equation (13) can be replaced with

$$\mathscr{L}^m(q) \equiv \mathscr{L}(q) - \frac{h}{2}\frac{\partial}{\partial x_j}\left(\beta_q \frac{u_j u_k}{|\mathbf{u}|}\frac{\partial q}{\partial x_k}\right) = 0, \tag{15}$$

where β_q is the state variable number-dependent dissipation level.

4. FREQUENCY ANALYSIS, BASIC PERFORMANCE

In one-dimensional cases, the finite difference von Neumann stability analysis is extended to arbitrary width stencils [18], admitting full theoretical prediction of comparative

performance of the range of GWS–TWS algorithms. The linear assumption focuses on the single Fourier semi-discrete mode

$$q^h_\omega(j\Delta x, t) = \exp[i\omega(j\Delta x - U(\omega)t)]. \tag{16}$$

The phase velocity Φ^h of the approximation is $U(\omega)$, where ω is the Fourier mode frequency, and the relative phase velocity is $U(\omega)/u$, where u is for the analytical solution. The associated amplification factor is

$$G^h \equiv \frac{Q^{n+1}_j}{Q^n_j} = \exp[-i\omega U(\omega)\Delta t] = \exp[-imC\Phi^h] \tag{17}$$

for time step Δt. For $U(\omega)$ real, the modulus of G^h is unity, hence the algorithm is non-dissipative.

Replacing ω by wavenumber $m = \omega\Delta x$ admits the expressed Courant number form in terms of Φ^h. Thereby, a solution for relative phase velocity is achieved as

$$\Phi^h = \frac{\tan^{-1}[\mathrm{Im}(G^h)/\mathrm{Re}(G^h)]}{-mC}, \tag{18}$$

where 'Im' and 'Re' denote imaginary and real parts respectively.

In [18], the relative velocity Φ^h and amplification factor modulus $|G^h|$ were calculated for the range of TWS and FD/FV algorithms for Courant numbers C between 0 and 1 and wavenumbers between 0 and π. The non-dissipative trapezoidal rule ($\theta = \frac{1}{2}$) was used for each time integration. Phase velocity results are summarized in Figure 1 for Courant numbers of $\frac{1}{8}$, $\frac{1}{2}$ and 1. All methods fail totally at $m = \pi$, which corresponds to the $2\Delta x$ mode, which cannot be propagated by a discrete method. Conversely, the $k = 1, 2, 3$ FE basis TWS (β, γ) algorithms can each propagate the entire spectrum at $C = 1$ via optimum selection of $\gamma(-\frac{1}{2}, -\frac{1}{15}, -\frac{1}{18}$ for $k = 1, 2, 3$ respectively). Across the Courant number spectrum, the Crank–Nicolsen (CN) FD and QUICK FV schemes are universally poorer performers than the $k = 1$ GWS–TWS algorithms and the $k = 2, 3$ GWS–TWS algorithms are each an improvement over $k = 1$.

The companion amplification factor modulus distributions are summarized in Figure 2 for $C = \frac{1}{2}$ for the various dissipative algorithms. The CN algorithm and each of the six FE GWS algorithms are non-diffusive and have an amplification factor modulus identically equal to unity. The amplification factor modulus at $C = \frac{1}{2}$ for the QUICK methods, and linear upwind finite difference method are each compared with dissipative linear basis β TWS FE methods with $\beta = \frac{1}{8}$, $\frac{1}{6}$ and $\frac{1}{3}$, which produce a comparable level of short-wavelength dissipation. Dissipation at wavenumbers approaching π contributes to stability, since $2\Delta x$ waves are damped accordingly. The linear upwind method also exhibits significant dissipation at wavenumbers as small as $\pi/4$, indicating that every solution component is heavily damped and accuracy is compromised. The trends in Figure 2 become more dissipative at larger Courant numbers.

Documentary computational experiments confirm these theoretical distinctions, and also help refine the $k = 1$ basis TWS algorithm for optimal performance based on phase velocity. The theory [18] generates a two-step method with $\gamma \to \gamma_1, \gamma_2$, with each optimized as a function of C. The resultant γ_α-TWS $k = 1$ algorithm maintain 1% phase accuracy on $0 < C \leq 1$, for $m \geq 3\pi/4$ in a tridiagonal algorithm. Figure 3 compares the range of algorithm performance for viscous propagation of a step function and non-viscous

propagation of a one-element wide square wave for $C = \frac{1}{4}, \frac{1}{2}, \frac{3}{4}$ and 1. Only the optimized $k = 1$, γ_α-TWS algorithm performance produces acceptable accuracy over the range.

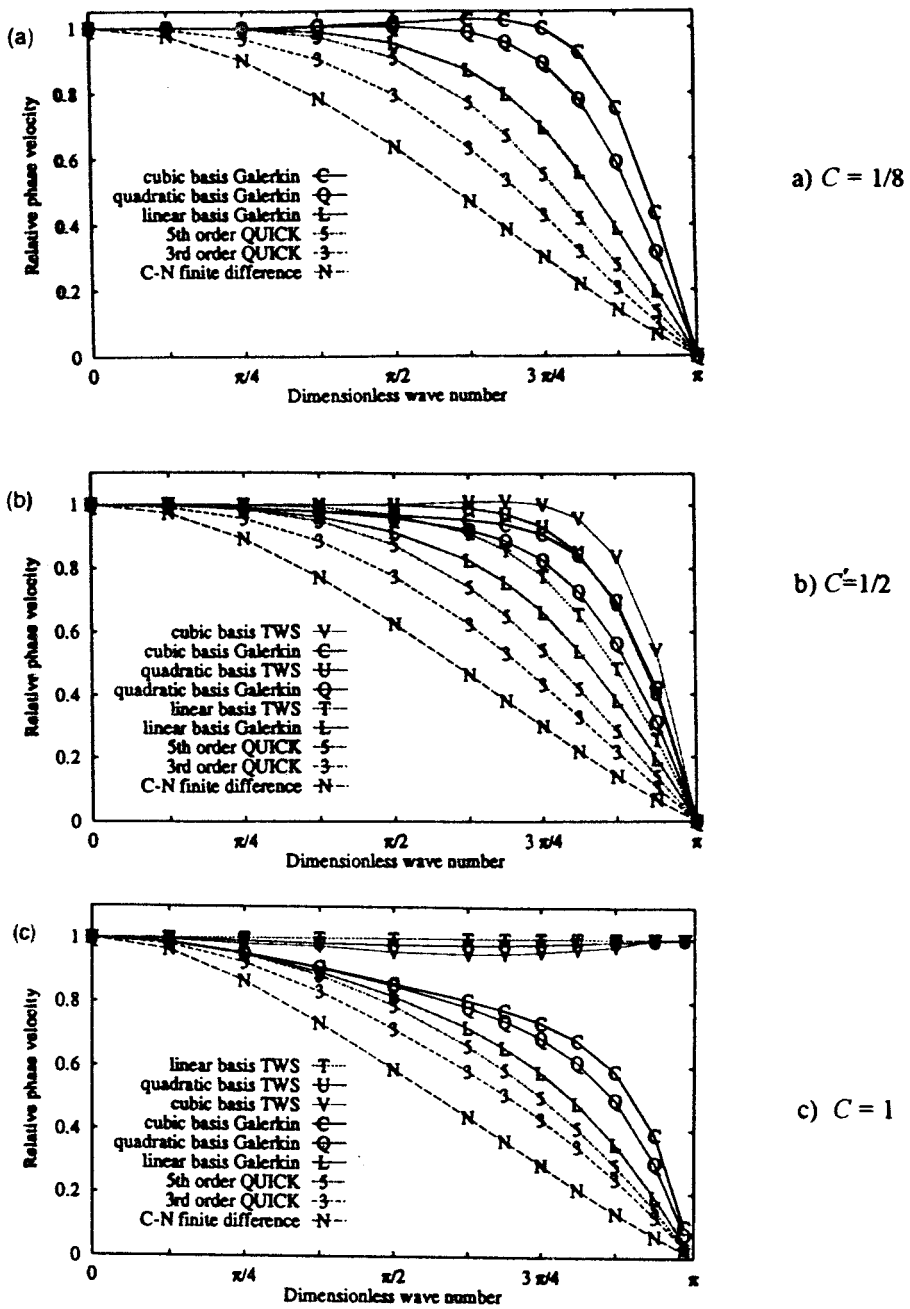

Figure 1. Phase velocity distributions of various GWS–TWS and FD/FV algorithms.

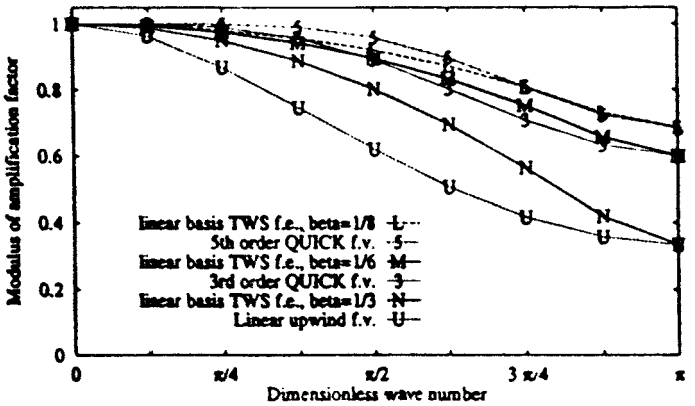

Figure 2. Amplification factor modulus for select dissipative algorithms at $C=\frac{1}{2}$.

5. MODIFIED EQUATION ANALYSIS, n-DIMENSIONS

The 'modified equation' analysis procedure, developed for finite difference methods [25], is extendible to GWS–TWS FE CFD methods. The $k=1$ basis recursion relation form for the fourth-order-accurate $n=1$ TWS algorithm with diffusion coefficient v is

$$\hat{\mathscr{L}}^h(Q)=\left(\frac{2+C^2}{12}(Q_{j+1}^{n+1}-Q_{j+1}^{n})+\frac{8-C^2}{12}(Q_j^{n+1}-Q_j^{n})+\frac{2-C^2}{12}(Q_{j-1}^{n+1}-Q_{j-1}^{n})\right)$$
$$+\frac{C^2}{4}(Q_{j+1}^{n+1/2}-Q_{j-1}^{n+1/2})-\frac{v}{2}(Q_{j+1}^{n+1/2}-2Q_j^{n+1/2}+Q_{j+1}^{n+1/2}). \tag{19}$$

The associated modified equation, where T denotes the *time* term and X^p denotes the p^h spatial derivative, is

$$T+CX=-vX^2-\frac{v(2C^2-1)}{12}X^4-\frac{C(6v^2-C^4-5C^2-4)}{720}X^5+\cdots. \tag{20}$$

The fourth-order accuracy (for $v=0$) previously predicted is thus confirmed in (20).

While Fourier analysis is tractable in one-dimensional cases, the modified equation analysis is readily extended to two- and three-dimensional cases. In two-dimensional form, the uniform mesh, θ implicit GWS $k=1$ basis algorithm modified equation is [24]

$$\begin{aligned}T+C_xX+C_yY=&\,2(2\theta-1)(C_x^2X^2+C_xC_yXY+C_y^2Y^2)\\&+8(-3\theta^2+3\theta-1)(C_x^3X^3+3C_x^2C_yX^2Y+3C_xC_y^2Y^2X+C_y^3Y^3)\\&+4(2\theta-1)(2\theta^2-2\theta+1)\\&\times(C_x^4X^4+4C_x^3C_yX^3Y+6C_x^2C_y^2X^2Y^2+4C_xC_y^3Y^3X+C_y^4Y^4)+\cdots.\end{aligned} \tag{21}$$

Stability properties are tenuous, as the second-order error term requires $\theta\geq\frac{1}{2}$ for positivity, which makes the fourth-order term also positive or zero. The third-order term cannot be eliminated by a real value of θ.

Stability is predictably improved for the $k=1$ basis TWS algorithm with the originally arbitrary directional coefficients β_{ij} and γ_{ij}. The resultant $n=2$ modified equation is [24]

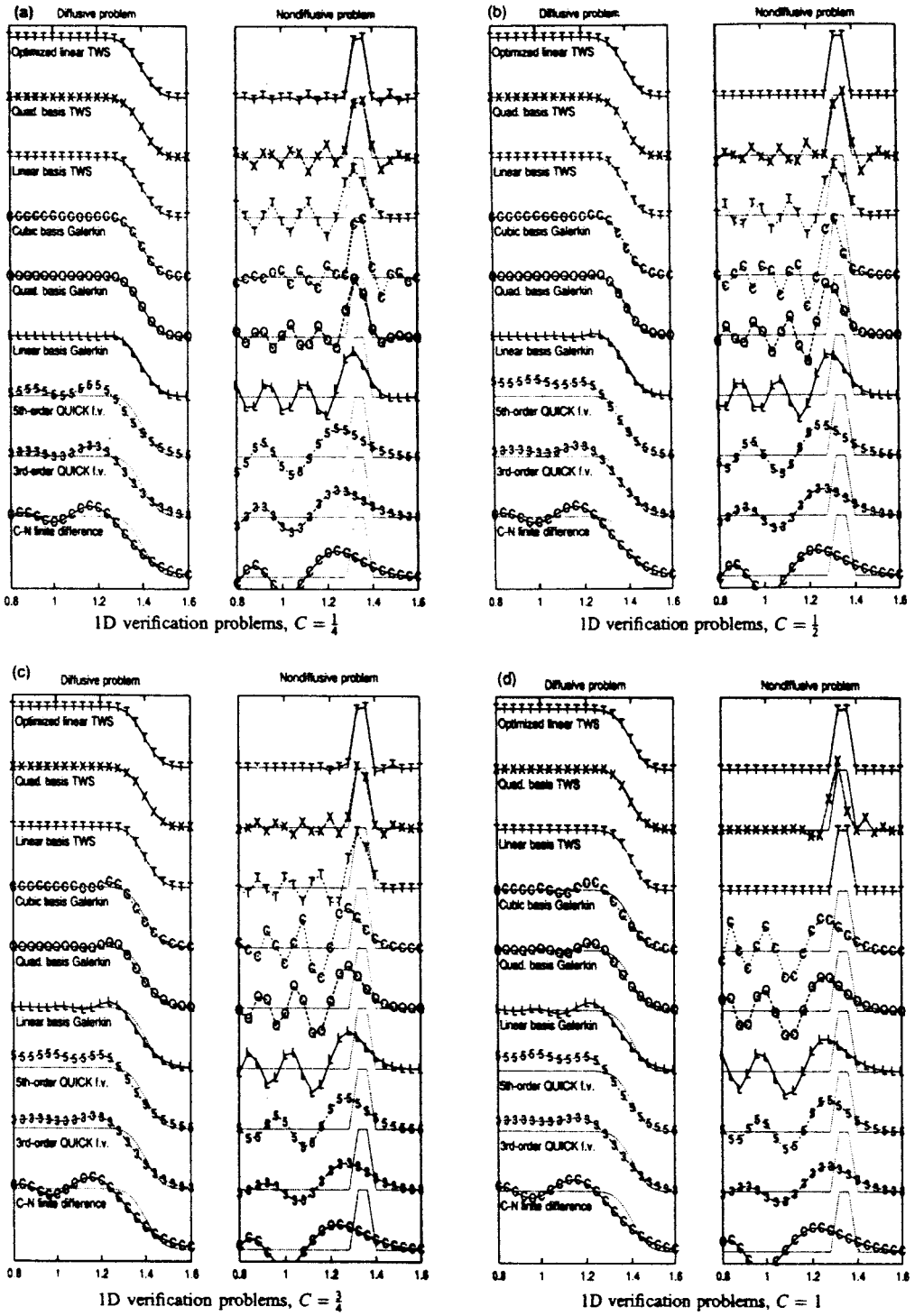

Figure 3. One-dimensional verification problems (from [18], Figure 6).

$$
\begin{aligned}
T + C_2X + C_2Y &= (\theta - \tfrac{1}{2})(C_x^2X^2 + 2C_xC_yXY + C_y^2Y^2) \\
&+ (\beta_{xx}C_x^2X^2 + \beta_{xy}C_xC_yXY + \beta_{yy}C_y^2Y^2) \\
&- C_x^3((\theta - 1)(\theta + \beta_{xx}) + \gamma_{xx} + \tfrac{1}{3})X^3 \\
&- C_x^2C_y((\theta - 1)(3\theta + \beta_{xx} + \beta_{xy}) + \gamma_{xx} + \gamma_{xy} + 1)X^2Y \\
&- C_y^2C_x((\theta - 1)(3\theta + \beta_{yy} + \beta_{xy}) + \gamma_{yy} + \gamma_{xy} + 1)XY^2 \\
&- C_y^3((\theta - 1)(\theta + \beta_{yy}) + \gamma_{xy} + \tfrac{1}{3})y^3 \\
&- C_x^4((\theta - 1)(\theta + \beta_{xx}) + \gamma_{xx} + \tfrac{1}{3} + \cdots),
\end{aligned} \tag{22}
$$

for which the third-order errors can be eliminated via

$$
\beta_{xx} = \beta_{xy} = \beta_{xy} = \frac{1}{2} - \theta + \varepsilon, \qquad \gamma_{xx} = \gamma_{yy} = \gamma_{xy} = \frac{1}{2} - \frac{\theta}{2} + \varepsilon(1 - \theta), \tag{23}
$$

for ε an arbitrary constant. The $n = 1$ fourth-order-accurate TWS algorithm is achieved by selecting $\varepsilon = 0$ and $\theta = \frac{1}{2}$. The comparable $n = 2$ TWS modified equation is

$$
\begin{aligned}
T + C_xX + C_yY = \varepsilon(C_x^2X^2 + 2C_xC_yXY + C_y^2Y^2) &+ \frac{C_x^2(C_x - 1)(C_x + 1)\varepsilon}{6}X^4 \\
&+ \frac{C_y^2(C_y - 1)(C_y + 1)\varepsilon}{6}Y^4 + \frac{C_xC_y(2C_x^2 - 1)\varepsilon}{3}X^3Y + \frac{C_xC_y(2C_y^2 - 1)\varepsilon}{3}Y^3X \\
&+ \frac{(6C_x^2C_y^2 - C_x^2 - C_y^2)\varepsilon}{6}X^2Y^2 + \cdots.
\end{aligned} \tag{24}
$$

For $\varepsilon > 0$, the method should be stable as second-order errors are positive. For $C_x < 1$ and $C_y < 1$, stability is enhanced as fourth-order errors along co-ordinates X^4Y^4 are negative. For $C_x < 1/\sqrt{2}$ and $C_y < 1/\sqrt{2}$, additional stability accrues as fourth-order errors along co-ordinates X^3Y, Y^3X are negative. For $C_x < 1/\sqrt{3}$ and $C_y < 1/\sqrt{3}$, stability is further enhanced as fourth-order errors along co-ordinates X^2Y are negative. Another TWS selection with $\theta = \frac{1}{2}$, which eliminates fourth-order errors, is [24]

$$
\beta_{xx} = \beta_{yy} = \beta_{xy} = \varepsilon, \qquad \gamma_{xx} = \frac{\varepsilon}{2} - \frac{1}{4} + \frac{1}{6}C_x^2, \qquad \gamma_{xx} = \varepsilon - \frac{1}{4}, \qquad \gamma_{xx} = \frac{\varepsilon}{2} - \frac{1}{4} + \frac{1}{6}C_y^2. \tag{25}
$$

Figure 4 confirms the GWS–TWS algorithm performance improvements for the classic rotating cone validation [17].

6. SHOCK CAPTURING, MONOTONICITY

As another approach to stability, distinct from the TWS formulation in theoretically requiring a monotone solution, the construction of a subgrid embedded (SGM) FE basis [21] addresses the fundamental issue of multi-dimensional *practical* (coarse) solution accuracy with guaranteed monotonicty and minimal (optimal) numerical diffusion. It is based on a genuinely non-linear, non-hierarchical basis for implementing GWS. Verification for both linear and non-linear convection–diffusion equation SGM finite element solutions is documented [22] for small ε ($O10^{-5}$) in (1) for which monotone and nodally accurate solutions are obtained on coarse grids.

The SGM basis is appropriate only for f_j^y in (1) [21]. The key efficiency ingredient is reduction to linear basis element matrix rank for any embedded degree via static condensation. The theory augments the diffusion term in (5) via an *embedded* function $g(x, c)$, hence the name 'SubGrid eMbedded'. The definite integral form of the resultant SGM basis (denoted $\{N_s\}$) matrix is

$$\int_{\Omega_e} \frac{\partial \{N_s\}}{\partial x} \frac{\partial \{N_s\}^T}{\partial x} \, \mathrm{d}x \Rightarrow \int_{\Omega_e} g(x, c) \frac{\partial \{N_k\}}{\partial x} \frac{\partial \{N_k\}^T}{\partial x} \, \mathrm{d}x \Bigg|^R, \tag{26}$$

where the statically condensed, reduced Rank form is denoted $|^R$. The embedded polynomial $g(x, c)$ contains at least one arbitrary parameter c for each co-ordinate direction and for each additional Lagrange degree $k \geq 2$. The resultant $n = 1$ linear model problem recursion relation yields a constraint on c for a monotone solution [22], which is specifically solution-dependent for the non-linear problem (1).

Performance of the SGM element is confirmed for numerous verifications and benchmarks for $n = 1, 2, 3$ [21,22]. Of particular note is the off-design de Laval nozzle shock benchmark problem [23], containing numerous subtle features. Figure 5 summarizes the essence of the comparative steady solutions obtained via TWS and SGM methodologies. The TWS solutions are monotone only for the shock smeared across three or more elements. Conversely, the SGM

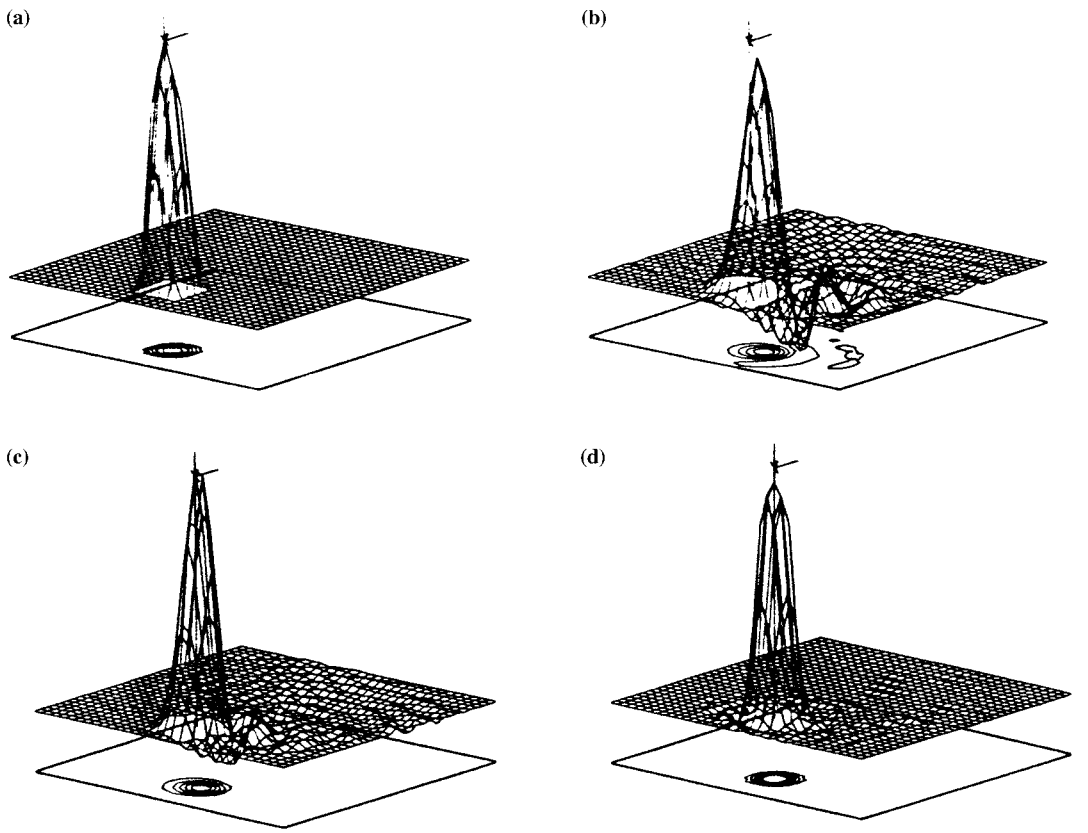

Figure 4. GWS–TWS $k = 1$ algorithm solutions for rotating cone, $\theta = 0.5$, $\bar{C} = 0.5$, (a) analytical, (b) GWS, (c) TWS, fourth-order, (d) TWS, phase optimized [24].

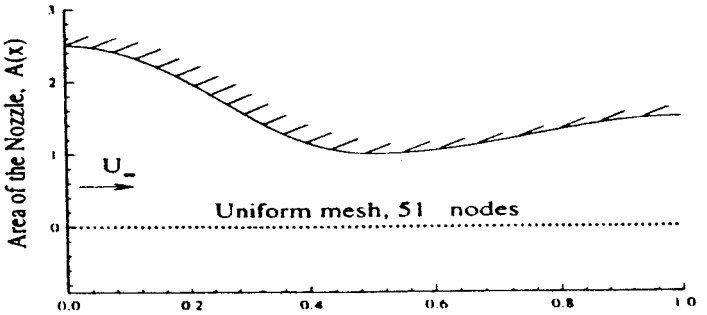

a) de Laval nozzle geometry

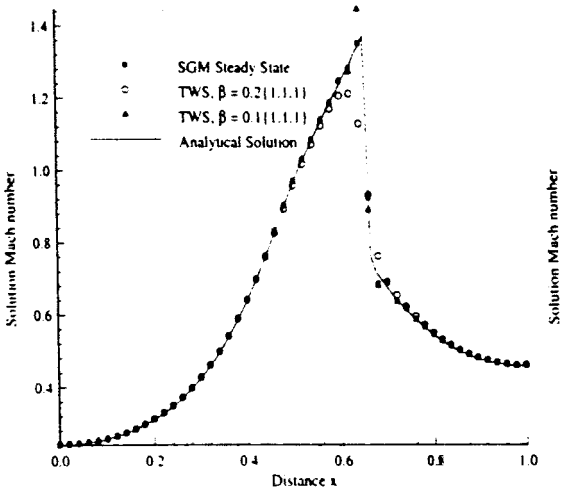

b) TWS and SGM comparison on uniform mesh

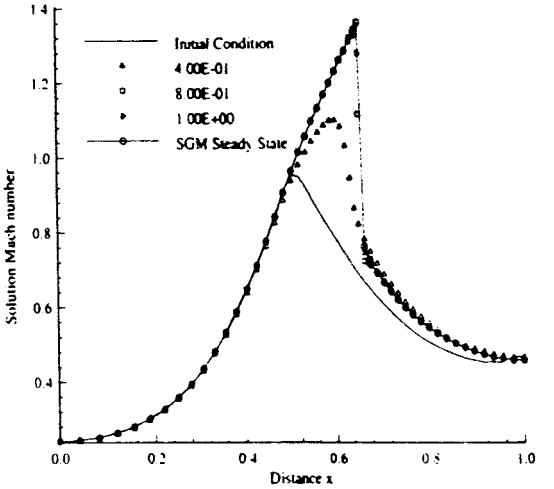

c) Time evolution of SGM solution

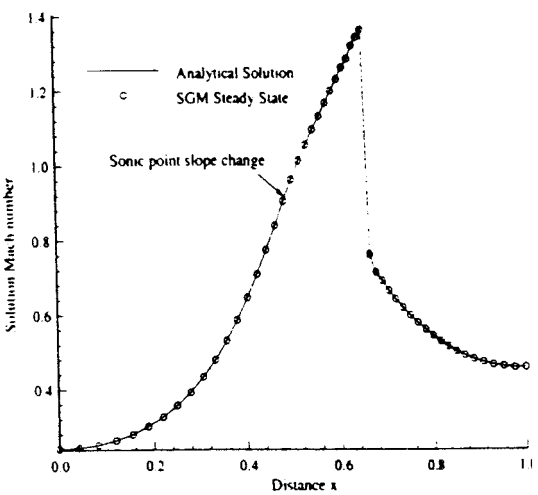

d) SGM solution on 51 node non-uniform mesh

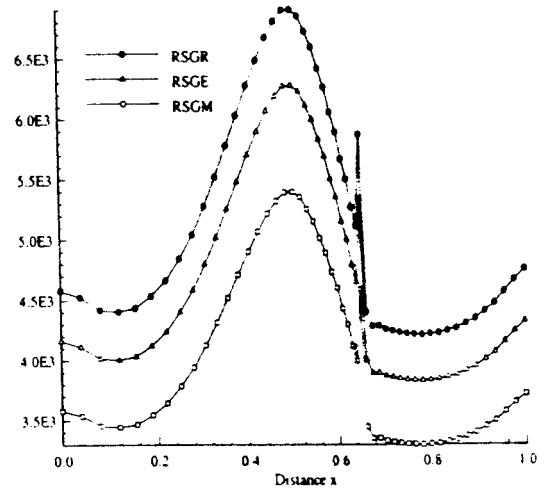

e) Steady state distributed SGM parameter $rsgm_q$

Figure 5. Steady state SGM solution distributions for transonic compressible flow, $Re = 10^6$.

solution captures the shock on one element and is *monotone*. The key to this performance is the distinct non-linear parameter estimation $c = c(q)$ for the state variable $q = (\rho, \rho u, E)$, denoted in Figure 5(e) as 'RSG', indicating a predicted sharp post-shock dissipation level critical to monotonicity.

A companion theory [26] has produced the non-linear element upstream weak statement (NEWS) algorithm, for the compressible Euler equations, as a characteristics-based replacement of the TWS formulation. The kinetic flux vector in (1) is replaced with

$$\mathbf{f}_j \equiv \mathbf{f}_j - \varepsilon\psi\left[c(\beta\, \mathbf{a}_j\mathbf{a}_l + \beta^N \mathbf{a}_j^N \mathbf{a}_l^N)\, \frac{\partial q}{\partial x_l} + a_j\left(\frac{\partial \mathbf{f}_l^q}{\partial x_l} + \delta\, \frac{\partial \mathbf{f}_l^p}{\partial x_l}\right)\right], \tag{27}$$

where the bracket contains the contraction of an upstream-bias tensor with the gradient of q. The first two terms denote the acoustics component, which for transonic Mach number is designed non-negligible only within a narrow multi-dimensional conical region about the cross-flow direction. The parentheses contain the convection and pressure decomposition of the kinetic flux vector $\mathbf{f}_j$.

The positive variables ε and ψ are a reference length and the upstream-bias 'smoothness' controller. In regions of solution smoothness, ψ decreases from unity, hence $\mathbf{f}^c$ approaches $\mathbf{f}_j$. The unit vectors $\mathbf{a} = \mathbf{a}(q)$ and $\mathbf{a}^N = \mathbf{a}^N(q)$ are parallel and perpendicular to the velocity, $c = c(q)$ denotes the local speed of sound and $\beta = \beta(M)$ and $\beta^N = \beta^N(M)$ are two Mach number-dependent upstream-bias functions. In the acoustics limit, $\beta(0) = \beta^v(0) = 1$, and $\beta(M) \equiv 0$ for $M \geq M_s$, where M_s denotes a subsonic threshold Mach number. Conversely, β^N remains positive and approaches zero as M increases, $\delta = \delta(M)$ is a scalar pressure-gradient influence function, with $0 \leq \delta(M) \leq 1$, $\delta(0)$ and $\delta(\mathrm{M}) = 1$ for $M = 1$. Figure 6 graphs these NEWS variables, which are analytically derivable [26].

In NEWS, the streamwise dissipation depends on Mach number, while the cross-flow dissipation decreases for increasing Mach number and becomes negligible for supersonic flows. The acoustics perturbation is important for accurate approximate acoustic wave propagation and is also pivotal for global stability. In fact, without acoustics perturbation, the characteristic eigenvalues turn negative, hence unstable. Figure 7 documents the NEWS performance for the supersonic compression ramp $Ma_\infty = 3.0$ validation problem. The oblique shock density solution is essentially non-oscillatory and freely crosses the outflow boundary without reflection.

7. CONCLUSIONS

Weak statement theory provides a rich basis for construction of CFD algorithms for the Navier–Stokes equations. The Taylor extension, coupled with the FE basis function is fundamental to the conversion to a stable computable form. Herein, GWS and various TWS formulations are documented for stability and accuracy for a range of traditional and non-traditional Lagrange basis forms, confirmed to control/annihilate short wavelength dispersion error pollution. In addition to providing a rational basis for CFD algorithm design, the TWS process recovers a range of schemes derived by alternative means within a rational hierarchical theory that provides guidance for the next level of development.

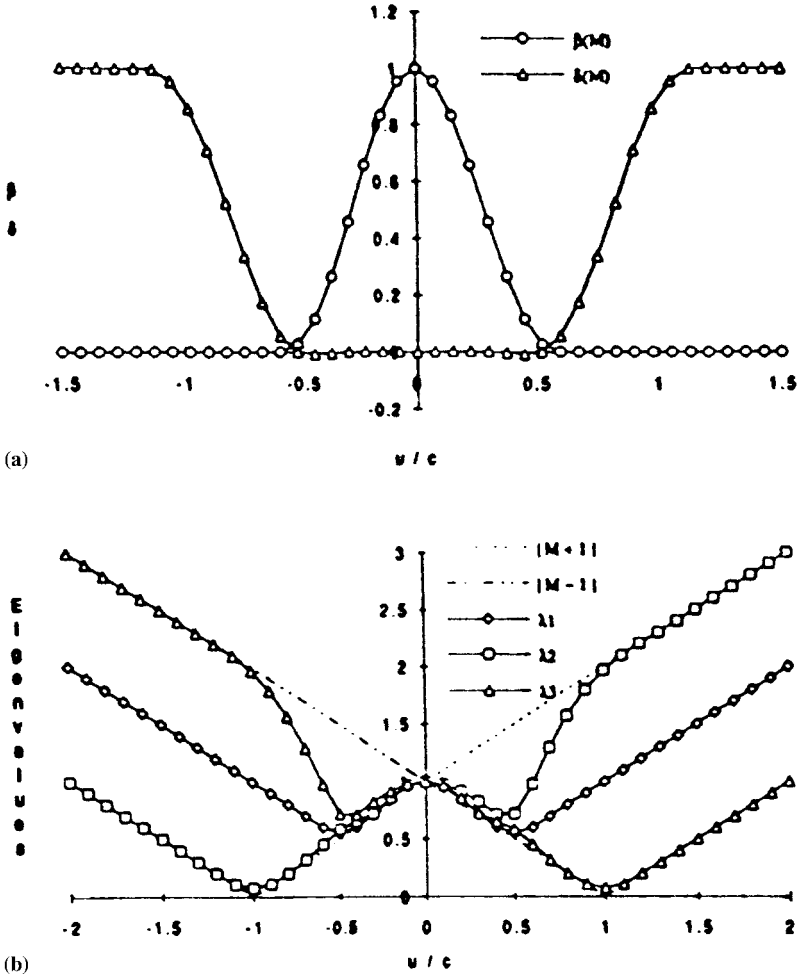

Figure 6. NEWS algorithm components, (a) upstream-bias functions β and δ, (b) upstream-bias streamwise eigenvalues.

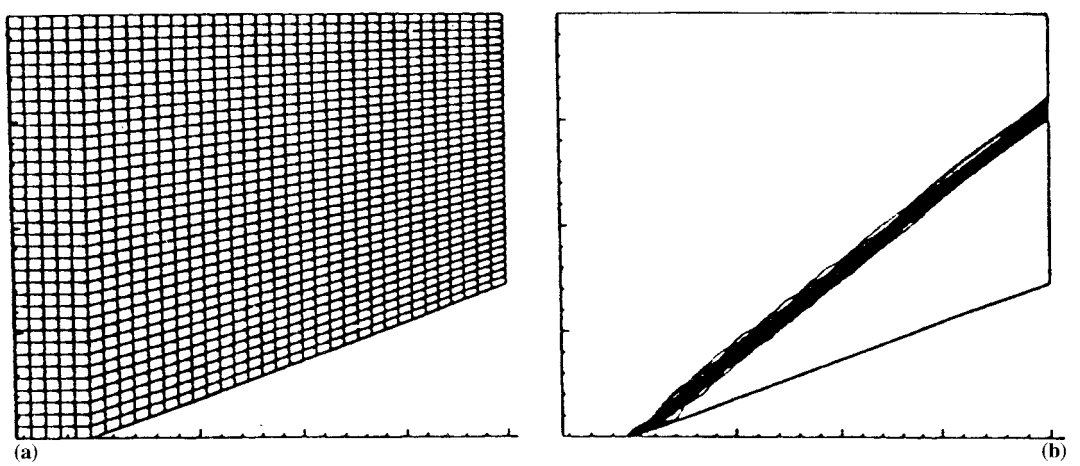

Figure 7. Compression ramp, $Ma_\infty = 3.0$ (a) 35×35 element grid, (b) NEWS solution density contours.

REFERENCES

1. A.J. Baker and J.W. Kim, 'A Taylor weak statement algorithm for hyperbolic conservation laws', *Int. J. Numer. Methods Fluids*, **7**, 489–520 (1987).
2. P.D. Lax, 'Weak solutions of nonlinear hyperbolic equations and their numerical computation', *Comm. Pure Appl. Math.*, **7**, 159–193 (1954).
3. H.O. Kreiss and J. Lorenz, *Initial-Boundary Value Problems and the Navier–Stokes Equations*, Academic Press, New York, 1989.
4. J.P. Boris and D.L. Book, 'Flux-corrected transport, I. SHASTA, a fluid transport algorithm that works', *J. Comput. Phys.*, **11**, 38–69 (1973).
5. S.T. Salezak, 'Fully multidimensional flux corrected algorithms for fluids', *J. Comput. Phys.*, **31**, 355–362 (1979).
6. B. van Leer, 'Flux vector splitting for the Euler equations', *Proceedings of the 8th International Conference on Numerical Methods in Fluid Dynamics*, Springer, Berlin, 1983.
7. H.T. Huynh, 'Accurate monotone cubic interpolation', *SIAM J. Numer. Anal.*, **30**, 57–100 (1993).
8. I. Babuska, B.Q. Guo and E.P. Stephan, 'On the exponential convergence of the hp version for boundary element Galerkin methods on polygons', *Math. Methods Appl. Sci.*, **12**, 413–427 (1990).
9. L. Demkowicz, A. Karafiat and J.T. Oden, 'Solution of elastic scattering problems in linear acoustics using hp boundary element method', *Comput. Methods Appl. Mech. Eng.*, **101**, 251–282 (1992).
10. S. Jensen, 'p version of mixed finite element methods for Stokes-like problems', *Comput. Methods Appl. Mech. Eng.*, **101**, 27–41 (1992).
11. C. Johnson and P. Hansbo, 'Adaptive finite element methods in computational mechanics', *Comput. Methods Appl. Mech. Engrg.*, **101**, 143–181 (1992).
12. J.T. Oden, 'Optimal hp finite element methods', *TICOM Report 92-09*, University of Texas, Austin, TX, 1992.
13. O.C. Zienkiewicz, D.W. Kelly, J. Gago and I. Babuska, 'Hierarchical finite element approaches, error estimates and adaptive refinement', in J. Whiteman (ed.), *The Mathematics of Finite Elements and Applications IV*, 1982, pp. 311–346.
14. O.C. Zienkiewicz and J.Z. Zhu, 'The super convergent patch recovery (SPR) and adaptive finite element refinement', *Comput. Methods Appl. Mech. Eng.*, **101**, 207–224 (1992).
15. J.T. Oden, 'Optimal hp finite element methods', *Comput. Methods Appl. Mech. Engrg.*, **112**, 309–331 (1994).
16. T.J.R Hughes, 'Multi-scale phenomena: Green's functions, the Dirichlet-to-Neumann formulation, subgrid scale models, bubbles and the origins of stabilized methods', *Comput. Methods Appl. Mech. Eng.*, **127**, 387–401 (1995).
17. A.J. Baker, *Finite Element Computational Fluid Dynamics*, Taylor & Francis, Washington, DC.
18. D.J. Chaffin and A.J. Baker, 'On Taylor weak statement finite element methods for computational fluid dynamics', *Int. J. Numer. Methods Fluids*, **21**, 273–294 (1995).
19. P. Lax and B. Wendroff, 'Systems of conservation laws', *Comm. Pure Appl. Math.*, **8**, 217–237 (1960).
20. J. Donea, 'A Taylor–Galerkin method for convective transport problems', *Int. J. Numer. Methods Eng.*, **20**, 101–119 (1984).
21. S. Roy, 'On improved methods for monotone CFD solution accuracy', *Ph.D. Dissertation*, The University of Tennessee, 1994.
22. S. Roy and A.J. Baker, 'A nonlinear subgrid embedded finite element basis for accurate monotone steady CFD solutions', *Int. J. Numer. Heat Transf.*, **31**, 135–176 (1997).
23. M.S. Liou and B. van Leer, 'Choice of implicit and explicit operators for the upwind differencing method', *Tech. AIAA 88-0624, 26th Aerospace Sciences Meeting*, 1988.
24. D.J. Chaffin, 'A Taylor weak statement finite element method for computational fluid dynamics', *Ph.D. Dissertation*, University of Tennessee, 1997.
25. R.F. Warming and B.J. Hyett, 'The modified equation approach to the stability and accuracy analysis of finite difference methods', *J. Comp. Phys.*, **14**, 159–179 (1974).
26. J. Iannelli, *AIAA 96-0763, 34th Aerospace Sciences Meeting*, 1996.

